Am J Transl Res 2019;11(4):1980-1996
www.ajtr.org /ISSN:1943-8141/AJTR0087803

Original Article

Shenkang injection, a modern preparation of Chinese patent medicine, diminishes tubulointerstitial fibrosis in obstructive nephropathy via targeting pericyte-myofibroblast transition

Yinglu Liu[1,2*], Ge Shi[3*], Hongyun Yee[1], Wenwen Wang[1], Wenbei Han[1], Buhui Liu[1], Wei Wu[2], Yue Tu[4], Qian Ma[2], Dongqin Huo[2], Ziyue Wan[5], Dongwei Cao[6], Yigang Wan[2]

[1]Department of Traditional Chinese Medicine, Nanjing Drum Tower Hospital Clinical College of Traditional Chinese and Western Medicine, Nanjing University of Chinese Medicine, Nanjing 210008, China; [2]Department of Traditional Chinese Medicine, Nanjing Drum Tower Hospital, The Affiliated Hospital of Nanjing University Medical School, Nanjing 210008, China; [3]Department of Nephrology, Wuhan First Hospital, Wuhan 430022, China; [4]Department of TCM Health Preservation, Second Clinic Medical School, Nanjing University of Chinese Medicine, Nanjing 210023, China; [5]Department of Social Work, Meiji Gakuin University, Tokyo 108-8636, Japan; [6]Department of Nephrology, Nanjing Drum Tower Hospital, The Affiliated Hospital of Nanjing University Medical School, Nanjing 210008, China. [*]Equal contributors.

Received November 2, 2018; Accepted January 26, 2019; Epub April 15, 2019; Published April 30, 2019

Abstract: Shenkang injection (SKI), a modern preparation of Chinese patent medicine, has been widely applied to clinical therapy in the chronic renal failure patients. However, it remains elusive whether SKI can ameliorate tubulointerstitial fibrosis (TIF) *in vivo*. Recently, pericyte-myofibroblast transition (PMT) plays an important role in the pathogenesis of TIF in obstructive nephropathy (ON). This report thus aims to demonstrate the therapeutic mechanisms of the dose-effects of SKI on TIF by targeting PMT and its signaling activation, compared with imatinib. All rats were divided into 5 groups, the sham-operated group, the vehicle-intervened group, the high dose of SKI-treated group, the low dose of SKI-treated group and the imatinib-treated group. The ON model rats were induced by unilateral ureteral obstruction (UUO), and administered with either the different doses of SKI or imatinib before and after modeling and for a period of 4 weeks. The changes before and after drugs intervention in TIF and PMT markers, and in platelet-derived growth factor receptor (PDGFR) and vascular endothelial growth factor receptor (VEGFR) signaling pathways activation in the kidneys were analyzed, respectively. As a result, PMT trigger was persistently accompanied with TIF exasperation in the obstructed kidneys after UUO, and that SKI definitely targeted PMT and significantly diminished TIF *in vivo*. In addition, the high dose of SKI, superior to imatinib, specifically blocked PMT through inhibiting the activation of PDGFR and VEGFR signaling in the kidneys of the UUO model rats. Overall, these findings may further suggest that targeting PMT can provide new strategies for ON treatment.

Keywords: Shenkang injection, tubulointerstitial fibrosis, pericyte-myofibroblast transition, platelet-derived growth factor receptor signaling pathway, vascular endothelial growth factor receptor signaling pathway, obstructive nephropathy

Introduction

It is now well recognized that the rate of progression of chronic kidney disease (CKD) correlates with the degree of renal fibrosis, especially tubulointerstitial fibrosis (TIF) in cortical, which is characterized by tubular atrophy, interstitial extracellular matrix (ECM) accumulation, inflammatory cell infiltration and fibroblast proliferation/differentiation in renal interstitium [1, 2]. Recently reported studies have highlighted an important role for renal pericytes in the pathogenesis of TIF in obstructive nephropathy (ON) induced by unilateral ureteral obstruction (UUO) [1, 3-8]. Renal pericytes are extensively branched cells embedded within capillary basement membrane, and stabilize vascular network through tissue inhibitor of metalloprotein-

ase (TIMP)-3 and the receptors of angiogenic growth factors including platelet-derived growth factor (PDGF) and vascular endothelial growth factor (VEGF) [3, 9]. Furthermore, renal pericytes detach from endothelial cells and migrate into tubulointerstitial space where they undergo a transition into myofibroblasts during the progression of TIF in CKD [6]. More importantly, the trigger of pericyte-myofibroblast transition (PMT) leads to microvascular rarefaction and TIF formation [10]. Therefore, blocking PMT in response to fibrotic injury has been identified as a new therapeutic target in the treatment of TIF.

PDGF receptor (PDGFR) signaling is made of four types of ligands including PDGF-A, -B, -C and -D and two receptors including PDGFRα and PDGFRβ. PDGFR possesses tyrosine kinase activity and can be autophosphorylated upon ligand binding. The components of PDGFR signaling system are expressed constitutively or inducibly in the kidney including pericytes, endothelial cells, tubular epithelial cells and interstitial cells [11]. In addition to PDGFR, VEGF receptor (VEGFR) signaling at endothelial cells induced soon after renal injury stimulates profibrotic factors in the kidney to activate PMT [4]. The increasing evidences in ON and ischemia-reperfusion injury have been shown that PDGFR signaling at pericytes and VEGFR signaling at endothelial cells play the cooperative role during PMT trigger and TIF formation *in vivo*. When either PDGFR signaling or VEGFR signaling is blocked by circulating soluble receptor ectodomains, microvascular rarefaction and TIF are markedly attenuated in the obstructed kidneys [12]. Hence, inhibiting the activation of PDGFR and VEGFR signalings is also considered as a prime therapeutic target in the trigger of PMT.

As is known to all, Chinese herbal compound preparations including the traditional oral preparations and the modern intravenous preparations [13, 14] have a unique therapeutic action in chronic diseases. Thereinto Shenkang injection (SKI, the local name in China), which is developed from the famous and experienced doctors in traditional Chinese medicine (TCM) and consist of the extracts from 4 medicinal plants: radix et rhizoma rhei (Dahuang, the local name in China), radix astragali (Huangqi, the local name in China), radix salviae miltiorrhizae (Danshen, the local name in China) and Flos carthami (Honghua, the local name in China), has been frequently used to treat TIF in chronic renal failure (CRF) patients for nearly 20 years in China [15]. At present, it has been approved by the China State Food and Drug Administration for the treatment of CRF as a modern intravenous preparation of Chinese patent medicine (Z20040110). Xu *et al*. and Yao *et al*. recently reported the preliminary high performance liquid chromatography (HPLC) fingerprint analysis of SKI, showing several types of bioactive compositions subjected to strict quality control in the production [16, 17]. In clinics, SKI can effectively ameliorate renal dysfunction and TIF for CKD patients at stage III to stage IV [15]. The preliminary pharmacological studies expounded that SKI can suppress renal fibrosis and oxidative stress in 5/6 nephrectomized rats through regulating transforming growth factor (TGF)-β/Smad3 and mitogen-activated protein kinase (MAPK) signaling pathways [18-20]. In addition, Xu *et al*. reported that SKI and its major active component emodin inhibit high glucose induced proliferation of rat messangial cells (RMCs) by inducing cell cycle arrest at G1 phase as well as cellular apoptosis via up-regulation of pro-apoptotic mediators bax and caspase activation [21]. However, up to present, there are still some important issues unresolved in the role of PMT in ON treated by SKI, for instance, whether SKI can improve TIF through targeting PMT and its signaling activation, and if yes, what are the underlying mechanisms involved *in vivo*.

Here, to address these important issues, we designed the animal experiments to examine the hypothesis that the dose-effects of SKI, compared to imatinib (PDGFR tyrosine kinase inhibitor) as an anti-fibrotic drug in the patients with nephrogenic systemic fibrosis in Denmark [22], may block PMT at pericytes of the model rats with UUO-induced TIF, and inhibit the activation of PDGFR and VEGFR signaling in the kidneys. Results in agreement with this hypothesis will suggest that blocking PMT is protective in TIF of ON.

Materials and methods

Preparation and quality control of SKI

SKI purchased from Xi'an Century Shenkang Pharmaceuticcal Industry Co., Ltd (Xi'an, China) is composed by the extracts from a defined

mixture of Chinese herbs as follows, radix et rhizoma rhei (*Rheum palmatum* L., Dahuang), radix astragali [*Astragalus membranaceus* (Fisch.) Beg. Huangqi], radix salviae miltiorrhizae (*Salvia miltiorrhiza* Bunge., Danshen) and Flos carthami (*Carthamus tinctorius* L., Honghua). One injection (20 ml) contains 6 g of the above extracts. The extracted method and productive process of SKI protected by the patent law of China are both subjected to strict quality control, and the main components are subjected to standardization. The batch number of SKI used in this study was 201607021. The quality of SKI was measured with fingerprint analysis by HPLC based on the report of Dr. Xu *et al*. and Dr. Yao *et al*. [16, 17]. The known bioactive components of anthraquinones including *Aloe-emodin* ($C_{15}H_{10}O_5$; CAS: 481-72-1), *Rhein* ($C_{15}H_8O_6$; CAS: 478-43-3), *Emodin* ($C_{15}H_{10}O_5$; CAS: 518-82-1), *Chrysophanol* ($C_{15}H_{10}O_4$; CAS: 481-74-3) and *Physcion* ($C_{16}H_{12}O_5$; CAS: 521-61-9) (Figure S1) in 5 batches exhibited high stability.

Animals, drug and reagents

All experiments were performed using male Sprague-Dawley (SD) rats weighing from 190 to 220 g, purchased from the Experimental Animal Center of Nanjing Drum Tower Hospital (Nanjing, China). They were allowed one week to acclimatize before the experiment. The experimental protocol was approved by the Animal Ethics Committee of Nanjing University Medical School. Imatinib was provided by Dalian Meilun Biological Technology Co., Ltd (Dalian, China) and solubilized in distilled water (DW) and administrated via gavage. Antibody against fibronectin (FN), collagen type IV (CIV), VEGFA, PDGFRα, PDGFRβ and phosphorylated PDGFRα and PDGFRβ (p-PDGFRα, p-PDGFRβ), α-smooth muscle actin (αSMA) and vimentin were purchased from Abcam (Cambridge, UK). Antibody against VEGFR2 and glyceraldehyde-3-phosphate dehydrogenase (GAPDH) were bought from Cell Signaling Technology (Beverly, MA, USA).

Experimental design

Twenty-five rats were divided into 5 groups, the sham-operated group (the Sham group), the vehicle-intervened group (the Vehicle group), the high dose of SKI-treated group (the H-SKI group), the low dose of SKI-treated group (the L-SKI group) and the imatinib-treated group (the Imatinib group). According to the previous studies [23], the model rats with TIF were established by UUO. The rats were firstly administered with the high dose of SKI (5 g/kg/d), the low dose of SKI (1 g/kg/d), imatinib (50 mg/kg/d) and DW (5 ml/kg/d) from day 1 to 13 at the beginning of the experiment, and then, underwent UUO on day 14 (Figure S2). The UUO in this experiment was performed as previously described [24]. The rats in the Sham group were only exposed the left kidney during the operation. Following the administration and operation, the same interventions were sequentially given to the rats in the SKI groups, the Imatinib group and the Vehicle group respectively, by daily, morning gastric gavage for 2 weeks. In clinics, 100 ml/d SKI is used to treat a 60 kg non-dialysis CRF patient. Based on the animal standard conversion formula, the effective amount of SKI in a rat is equivalent to 5 g/kg/d. The dose of imatinib was referred to Elmholdt *et al*.' report [23]. At the end of 4 weeks after the administration, all rats were anesthetized by intraperitoneal injection of ketamine and sacrificed via cardiac puncture. The kidneys and the samples of urine and blood were collected for the detection of various indicators.

Blood biochemical parameters

Blood sampling from the heart was obtained from each rat during sacrifice. Plasma samples were processed for the determination of serum creatinine (Scr), blood urea nitrogen (BUN) and albumin (Alb). They were determined by automatic biochemical analyzer in Department of Laboratory Medicine of Nanjing Drum Tower Hospital.

Urinary protein and urinary N-acetyl-beta-D-glucosaminidase

All rats were weighed and placed in metabolic cages on days 0, 14 and 28. They were fasting and only allowed to drink water. Then the collected urine samples were used for detecting 24 h urinary protein (Upro) and urinary *N*-acetyl-beta-*D*-glucosaminidase (UNAG), which was determined with the method of chromatometry performed as previously described [25].

Renal histomorphometry

Periodic acid-Schiff (PAS) staining and Masson staining were performed as previously de-

scribed [26]. The rates of ECM and collagen in renal interstitial area were calculated with Image-Pro Plus (IPP) 6.0 software (Media Cybernetic). The results were confirmed by the pathological professional doctor.

Renal immunohistochemistry

Immunohistochemical staining was performed on 4-μm-thick paraffin-embedded renal sections as previously described [27]. Briefly, renal sections were stained by anti-FN, anti-CIV, anti-αSMA, anti-PDGFRβ and anti-vimentin antibodies (Serotec, Oxford, UK), respectively, and then detected by EnVision/horseradish peroxidase (HRP) Kit (Dako, Carpinteria, CA). The rates of positive staining in renal interstitial area were also calculated with IPP 6.0 software (Media Cybernetic). The results were also confirmed by the pathological professional doctor.

Western blot

Western blot (WB) analysis was performed as previously described [28]. Renal tissues from the rats were isolated with phosphate-buffered saline including protease inhibitors (PI) and sequentially solubilized with 1% Triton X-100, RIPA buffer [0.1% sodium dodecyl sulfate (SDS), 1% sodium deoxycholate, 1% Triton X-100, 0.15 mol/L NaCl, and 0.01 mol/L ethylenediaminetetraacetic acid in 0.025 mol/L Tris-HCl, pH 7.2] with PI, and separated into Triton X-100-soluble (T), RIPA-soluble (R) and RIPA-insoluble (S) fractions. The RIPAI-insoluble fraction was solubilized with sodium dodecyl sulfate-polyacrylamide gel electrophoresis (SDS-PAGE) sample buffer (2% SDS, 10% glycerol and 5% 2-mercaproethanol in 0.0625 mol/L Tris-HCl, pH 6.8) (S fractions). Equal amounts of these sequentially solubilized fractions were subjected to SDS-PAGE with 7.5% or 10% acrylamide gel, and transferred onto a polyvinylidene fluoride membrane (Bio-Rad, Hercules, CA, USA) by electrophoretic transblotting for 30 minutes using Trans-Blot SD (Bio-Rad). After blocking with BSA, the strips of membrane were exposed to anti-αSMA, vimentin, VEGFA, VEGFR2, PDGFRα, PDGFRβ, p-PDGFRα, p-PDGFRβ and GAPDH antibodies, respectively. They were washed and incubated with peroxidase-conjugated secondary antibodies for 1 h at room temperature. The bands were visualized by employing an alkaline phosphatase chromogen kit (5-bromo-4-chloro-3-indolil phosphate p-toluidine salt/nitro blue tetrazolium; Biomedica, AG, Staad, Switzerland). The density of the positive bands was quantitated by Densitograph (ATTO, Tokyo, Japan). The ratio of the densitometric signal of the molecules examined to that of GAPDH was determined. The data are shown as ratios relative to control findings and expressed as mean ± S.E. of 3 independent experiments.

Statistics

The differences among groups were analyzed by one-way analysis of variance (ANOVA), LSD method was used for multiple comparison. $P < 0.05$ was considered statistically significant. Values were expressed as means ± S.E. Qualitative data were analyzed using Fisher's exact test as indicated.

Results

TIF is induced in the obstructed kidneys after UUO

To investigate the pathomorphological characteristics of TIF in rats with ON induced by UUO, we firstly compared the appearances of kidneys and the changes of ECM and collagen in renal interstitium between the right non-ligated kidneys (NLKs) and the left ligated kidneys (LKs) in the UUO model rats. As shown in **Figure 1**, like the normal kidneys (NKs) of the Sham group rats (**Figure 1A**), the NLKs of the UUO model rats were integral, red and smooth (**Figure 1B**), and did not exhibit any pathomorphological alterations. In contrast, the LKs of the UUO model rats were significantly enlarged, hydrops and cyanodema on the surface (**Figure 1C**), and showed the serious hydronephrosis and the typical features of TIF including tubular atrophy, inflammatory cells infiltration, ECM accumulation and collagen deposition in renal interstitial area (**Figure 1F**, **1I-K**) on day 14 after UUO. Here, the significant increased scores of ECM and collagen of the LKs in the UUO model rats were detected, respectively. And compared with those of the NLKs in the UUO model rats or the NKs in the Sham group rats, the differences were statistically significant, respectively ($P < 0.01$) (**Figure 1L**, **1M**).

Then, we observed the immunohistochemical staining of fibrotic markers FN and CIV between the NLKs and the LKs of the UUO model rats. As

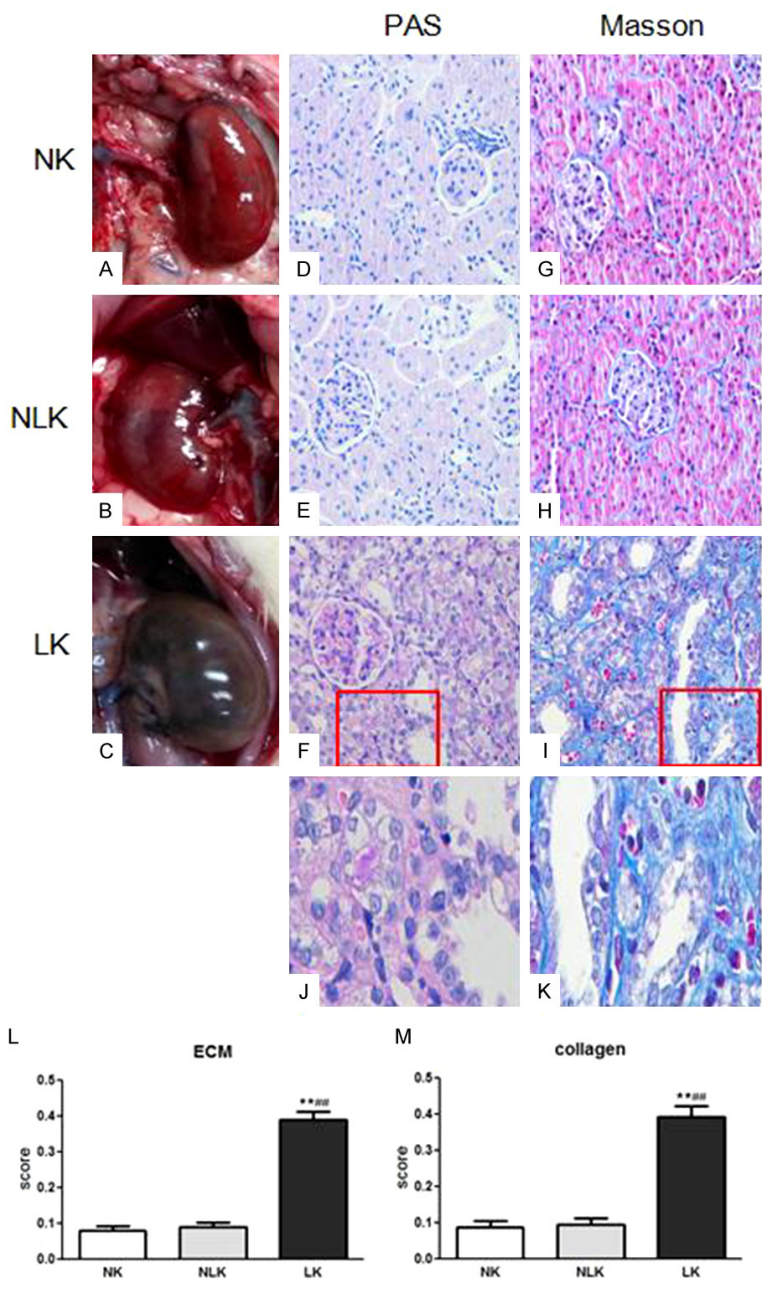

Figure 1. The kidney appearances and renal pathomorphological characterizations in the UUO model rats. The appearances of the normal kidneys (NKs) in the Sham group rats (A), the right non-ligated kidneys (NLKs) in the UUO model rats (B) and the left ligated kidneys (LKs) in the UUO model rats (C); The photomicrographs of PAS staining of the NKs in the Sham group rats (D), the NLKs in the UUO model rats (E) and the LKs in the UUO model rats (F, J); The photomicrographs of Masson staining of the NKs in the Sham group rats (G), the NLKs in the UUO model rats (H) and the LKs in the UUO model rats (I, K); The scores of ECM (L) and collagen (M) in renal interstitium. The LKs of the UUO model rats are significantly enlarged, hydrops and cyanodema on the surface, and show the serious hydronephrosis and the typical features of TIF including tubular atrophy, inflammatory cells infiltration, ECM accumulation and collagen deposition in renal interstitial area. Original magnification: × 400 (D-I). The data are expressed as mean ± S.E. (n = 5). $^{**}P < 0.01$ vs. the NKs in the Sham group rats; $^{\#\#}P < 0.01$ vs. the NLKs in the UUO model rats on day 14 after UUO.

shown in **Figure 2**, the NLKs of the UUO model rats presented the slight expressions of FN and CIV, which were limited to tubular basement membranes, whereas no significant immunostaining was found in renal interstitium (**Figure 2B**, **2F**). In comparison with the NLKs of the UUO model rats and the NKs of the Sham group rats, the LKs of the UUO model rats showed the intense expressions of FN and CIV accompanied by a strong immunostaining in renal interstitium (**Figure 2C**, **2D**, **2G**, **2H**). Moreover the positively stained areas of FN and CIV expressions by the immunohistochemical quantifying revealed the significant higher levels in the LKs of the UUO model rats than those in the NLKs of the UUO model rats or in the NKs of the Sham group rats, and the differences were statistically significant, respectively ($P < 0.01$) (**Figure 2I**, **2J**).

Taken together, these results indicated that TIF could be persistently induced in the obstructed kidneys of the UUO model rats, which was concretely characterized by tubular atrophy, ECM accumulation and collagen deposition in renal interstitium, as well as the intense expressions of FN and CIV.

PMT is triggered in the obstructed kidneys after UUO

To confirm the trigger of PMT in the obstructive kidneys after UUO, we examined the expressions of PMT markers including PDGFRβ, αSMA and vimentin in renal interstitium between the NLKs and the LKs of the UUO model rats by immunohistochemistry and WB analysis. The associated

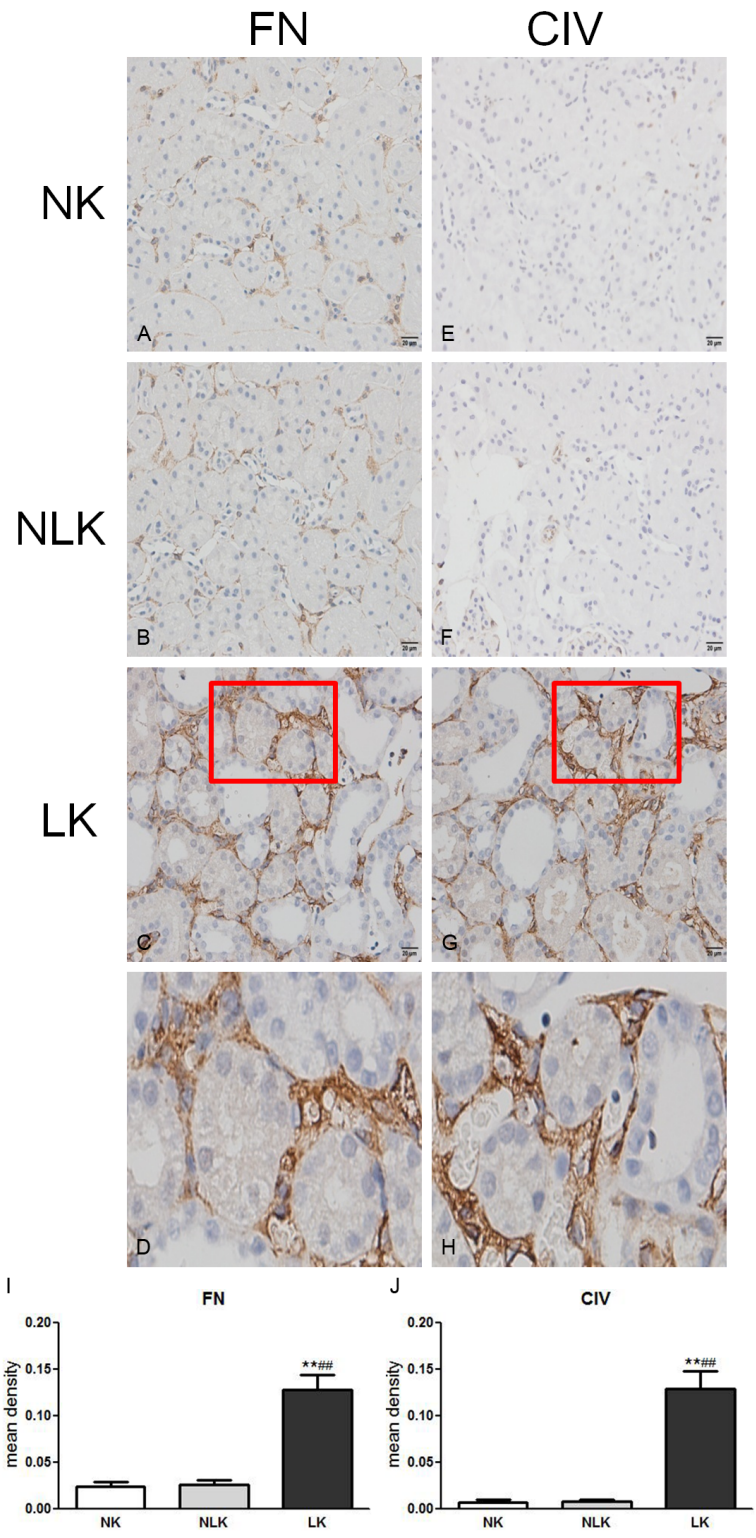

Figure 2. The expressional characterizations of FN and CIV in renal interstitium of the UUO model rats. The immunohistochemical staining of FN in renal interstitium of the normal kidneys (NKs) in the Sham group rats (A), the right non-ligated kidneys (NLKs) in the UUO model rats (B) and the left ligated kidneys (LKs) in the UUO model rats (C, D); The immunohistochemical staining of CIV in renal interstitium of the NKs in the Sham group rats (E), the NLKs in the UUO model rats (F) and the LKs in the UUO model rats (G, H); The immunohistochemical staining density scores of FN (I) and CIV (J) in renal interstitium. The LKs of the UUO model rats show the intense expressions of FN and CIV accompanied by a strong immunostaining in renal interstitium. Original magnification: × 400 (A-C and E-G). The data are expressed as mean ± S.E. (n = 5). $^{**}P < 0.01$ vs. the NKs in the Sham group rats; $^{\#\#}P < 0.01$ vs. the NLKs in the UUO model rats on day 14 after UUO.

immunodetections of PDGFRβ, αSMA and vimentin are assessed as the markers of PMT in the kidney [4]. As shown in **Figure 3**, like the NKs of the Sham group rats (**Figure 3A**), PDGFRβ positive immunostaining was confined to microvascular walls and tubular basement membranes, and absent in renal interstitial area of the NLKs in the UUO model rats (**Figure 3B**). In contrast, in the LKs of the UUO model rats, PDGFRβ positive immunostaining was additionally expressed by peritubular pericytes and renal interstitial cells as confirmed by the immunohistochemical quantifying (**Figure 3C**, **3D**). With the corresponding, the higher level of PDGFRβ protein expression was significantly detected in the LKs of the UUO model rats when compared with the NLKs of the UUO model rats or the NKs of the Sham group rats, and the differences were statistically significant, respectively ($P < 0.01$) (**Figure 4A**). The presence of renal interstitial cells expressing mesenchymal markers, such as αSMA and vimentin has been described as the additional source of generating PMT in ON [29, 30]. Thus the expressions of αSMA in peritubular pericytes and vimentin in myofibroblasts were also evaluated as the markers of PMT. As also shown in **Figure 3**, the immunohisto-

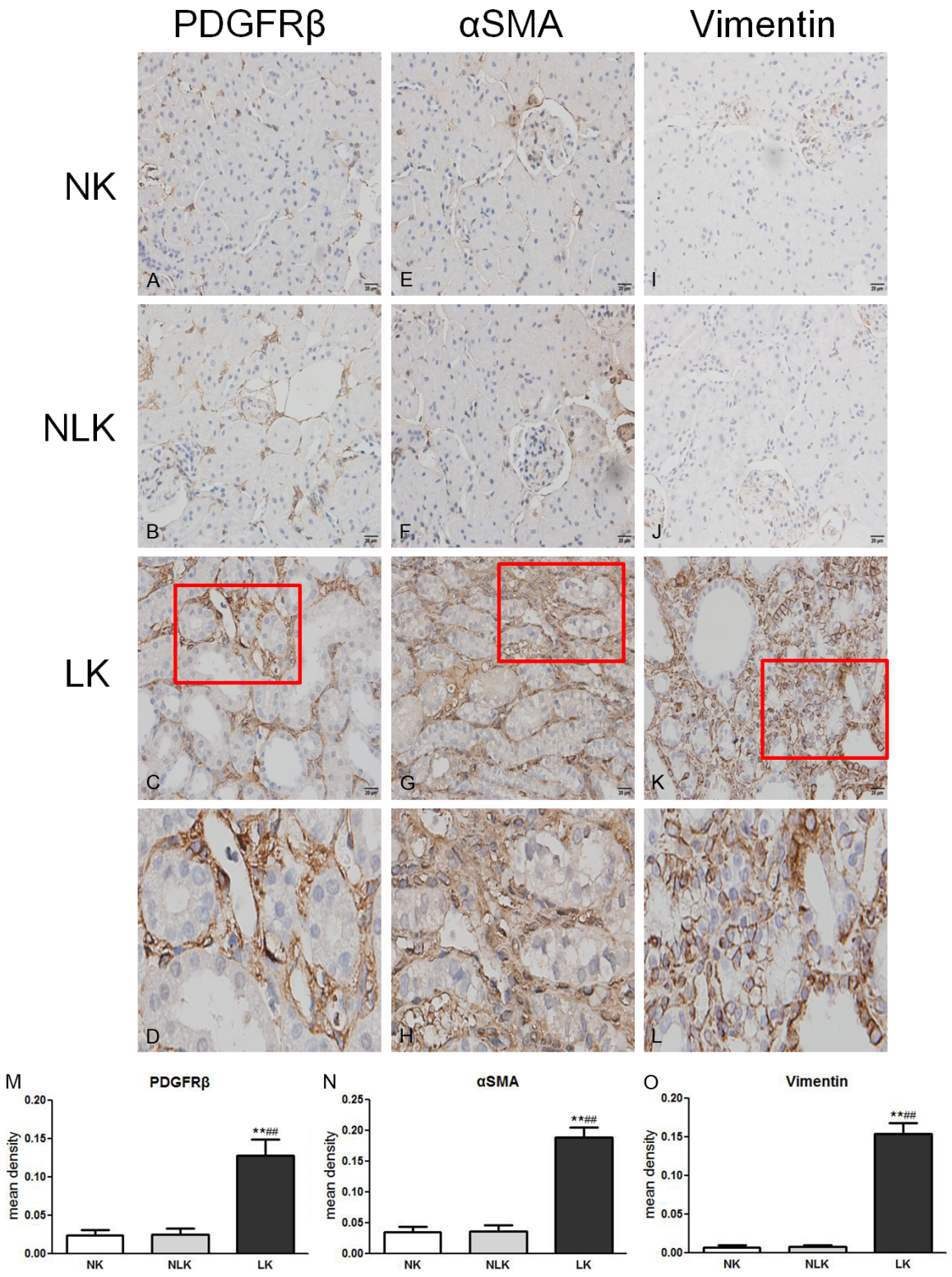

Figure 3. The expressional characterizations of PDGFRβ, αSMA and vimentin in renal interstitium of the UUO model rats. The immunohistochemical staining of PDGFRβ in renal interstitium of the normal kidneys (NKs) in the Sham group rats (A), the right non-ligated kidneys (NLKs) in the UUO model rats (B) and the left ligated kidneys (LKs) in the UUO model rats (C, D); The immunohistochemical staining of αSMA in renal interstitium of the NKs in the Sham group rats (E), the NLKs in the UUO model rats (F) and the LKs in the UUO model rats (G, H); The immunohistochemical staining of vimentin in renal interstitium of the NKs in the Sham group rats (I), the NLKs in the UUO model rats (J)

and the LKs in the UUO model rats (K, L); The immunohistochemical staining density scores of PDGFRβ (M), αSMA (N) and vimentin (O) in renal interstitium. The increased expressions of PDGFRβ, αSMA and vimentin in peritubular pericytes are detected in the obstructed kidneys of the UUO model rats. Original magnification: × 400 (A-C, E-G, I-K). The data are expressed as mean ± S.E. (n = 5). $^{**}P < 0.01$ vs. the NKs in the Sham group rats; $^{\#\#}P < 0.01$ vs. the NLKs in the UUO model rats on day 14 after UUO.

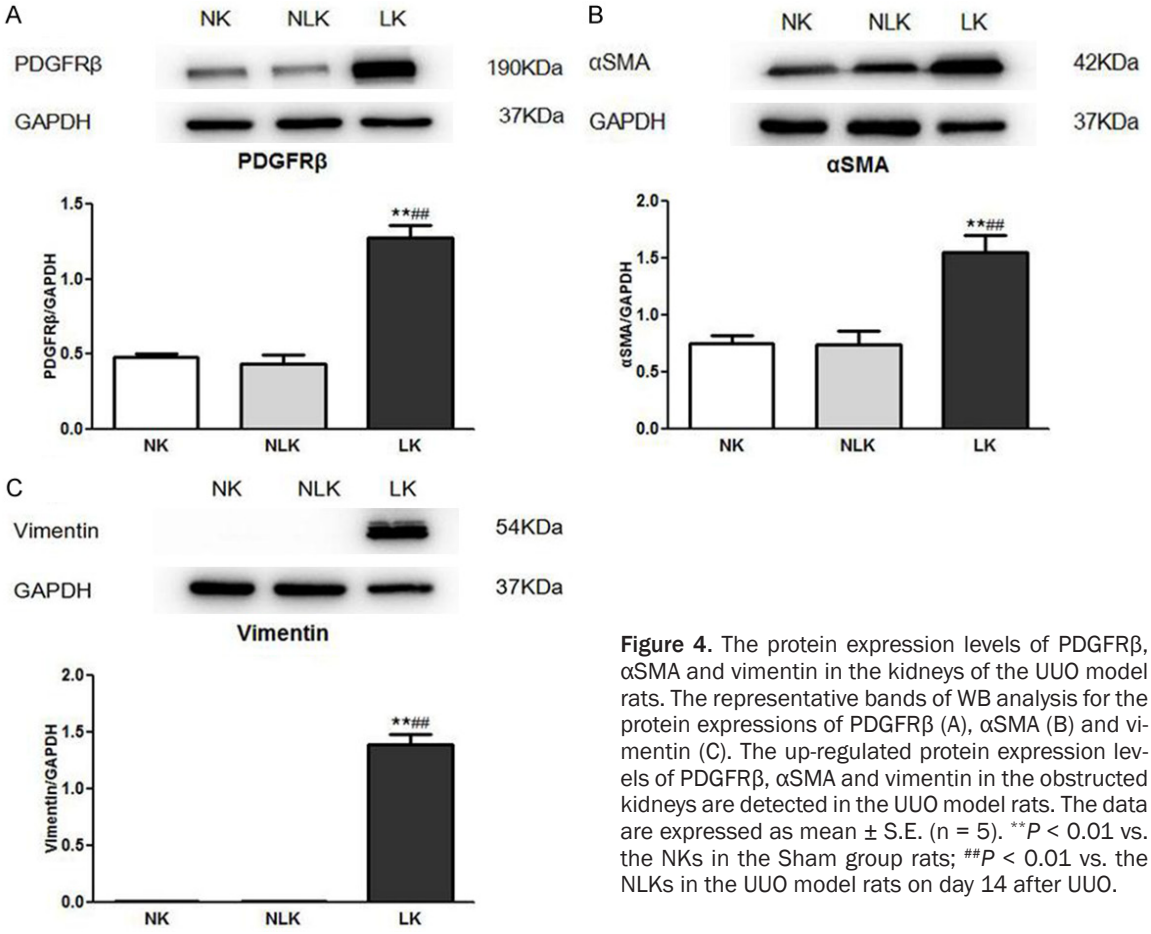

Figure 4. The protein expression levels of PDGFRβ, αSMA and vimentin in the kidneys of the UUO model rats. The representative bands of WB analysis for the protein expressions of PDGFRβ (A), αSMA (B) and vimentin (C). The up-regulated protein expression levels of PDGFRβ, αSMA and vimentin in the obstructed kidneys are detected in the UUO model rats. The data are expressed as mean ± S.E. (n = 5). $^{**}P < 0.01$ vs. the NKs in the Sham group rats; $^{\#\#}P < 0.01$ vs. the NLKs in the UUO model rats on day 14 after UUO.

chemical staining of αSMA and vimentin was performed in the NLKs and the LKs of the UUO model rats, as well as in the NKs of the Sham group rats. Our data showed that, similar to the NKs of the Sham group rats (**Figure 3E**, **3I**), the positive immunostaining of αSMA and vimentin was restricted to vascular walls and tubular basement membranes in like manner, and did not detect in renal interstitium in the NLKs of the UUO model rats (**Figure 3F**, **3J**). However, like the renal interstitial cells expressing PDGFRβ, a number of peritubular pericytes and renal interstitial cells with the positive immunostaining of αSMA or vimentin were found in renal interstitium in the LKs of the UUO model rats, respectively (**Figure 3G**, **3H**, **3K**, **3L**). In agreement with αSMA and vimentin expressions in renal interstitial area, WB analysis similarly revealed the significant increased levels of αSMA and vimentin protein expressions in the LKs of the UUO model rats when compared with those in the NLKs of the UUO model rats or the NKs of the Sham group rats, and the differences were statistically significant, respectively ($P < 0.01$) (**Figure 4B**, **4C**).

In short, these results indicated that PMT could be definitely triggered in the obstructed kidneys of the UUO model rats, which was concretely marked by the increased expressions of PDGFRβ, αSMA and vimentin in peritubular pericytes.

TIF aggravated by PMT is improved by SKI and imatinib after UUO

To clarify whether TIF was aggravated by PMT and could be improved by SKI and imatinib,

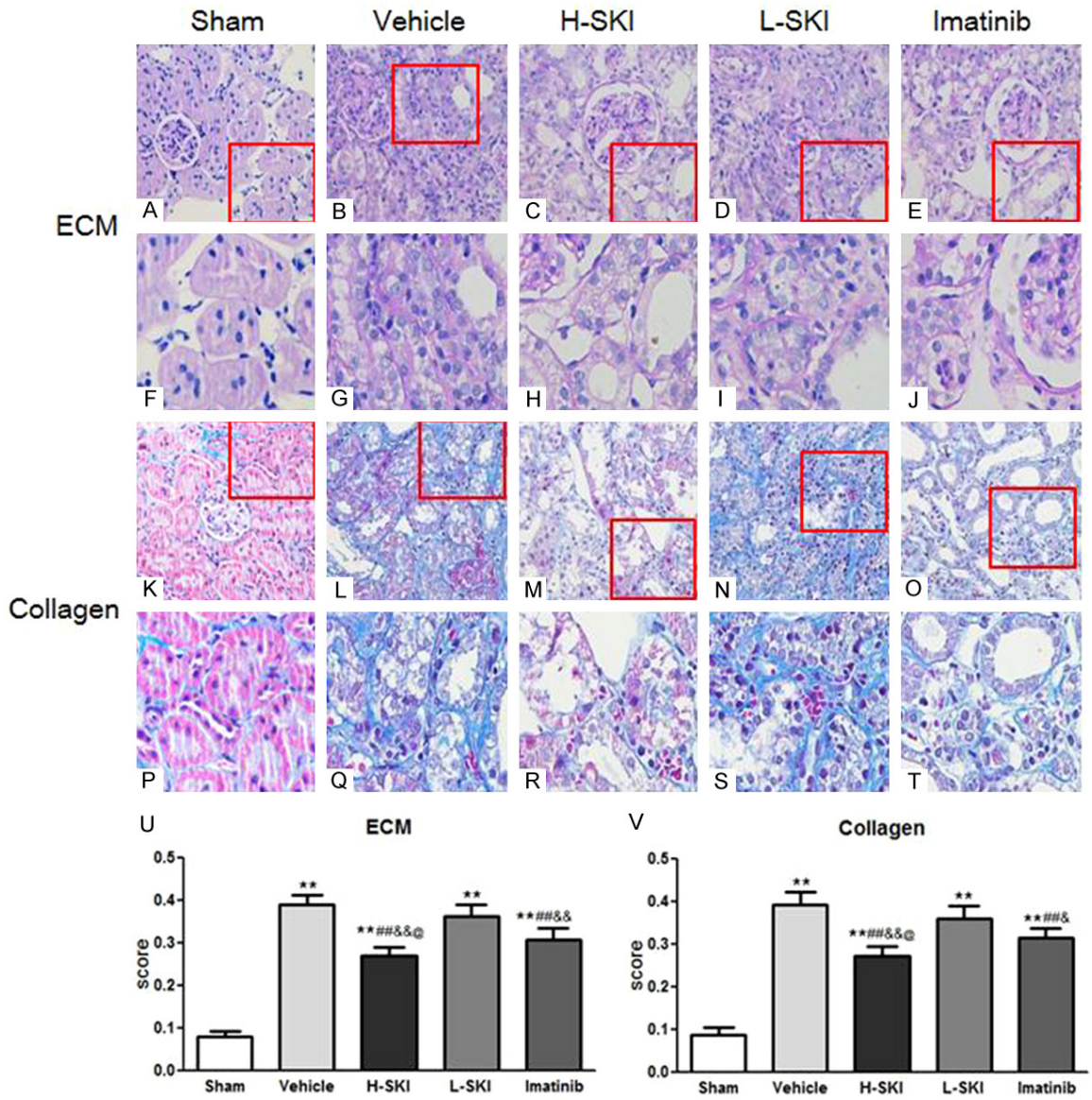

Figure 5. The effects of SKI and imatinib on the changes of ECM and collagen in renal interstitium of the ligated kidneys after UUO. The PAS staining of ECM (A-J) and the Masson staining of collagen (K-T) in renal interstitium among 5 group rats; The scores of ECM (U) and collagen (V) in renal interstitium among 5 group rat. ECM accumulation and collagen deposition in the LKs of the Vehicle group rats are increased, respectively, but significantly decreased in the LKs of both the H-SKI group rats and the Imatinib group rats. Original magnification: × 400 (A-E and K-O). The data are expressed as mean ± S.E. (n = 5). $^{**}P < 0.01$ vs. the Sham group rats; $^{\#\#}P < 0.01$ vs. the Vehicle group rats; $^{\&}P < 0.05$, $^{\&\&}P < 0.01$ vs. the L-SKI group rats; $^{@}P < 0.05$ vs. the Imatinib group rats on day 14 after UUO.

which is an anti-fibrotic drug in clinics [22], in the rats with UUO-induced obstructed renal injury, we assessed the changes in ECM and collagen of renal interstitium, as well as the immunohistochemical staining of PMT markers including PDGFRβ, αSMA and vimentin in peritubular pericytes among 5 group rats, especially between the different doses of the SKI-treated group rats and the imatinib-treated group rats. As shown in **Figure 5**, when compared with the NKs of the Sham group rats, we found that ECM accumulation (**Figure 5B**, **5G**) and collagen deposition (**Figure 5L**, **5Q**) in the LKs of the Vehicle group rats were increased, respectively, but significantly decreased in the LKs of both the H-SKI group rats (**Figure 5C**, **5H**, **5M**, **5R**) and the Imatinib group rats (**Figure 5E**, **5J**, **5O**, **5T**). And that, the statistical significant differences of these changes between the H-SKI group rats and the Imatinib group rats

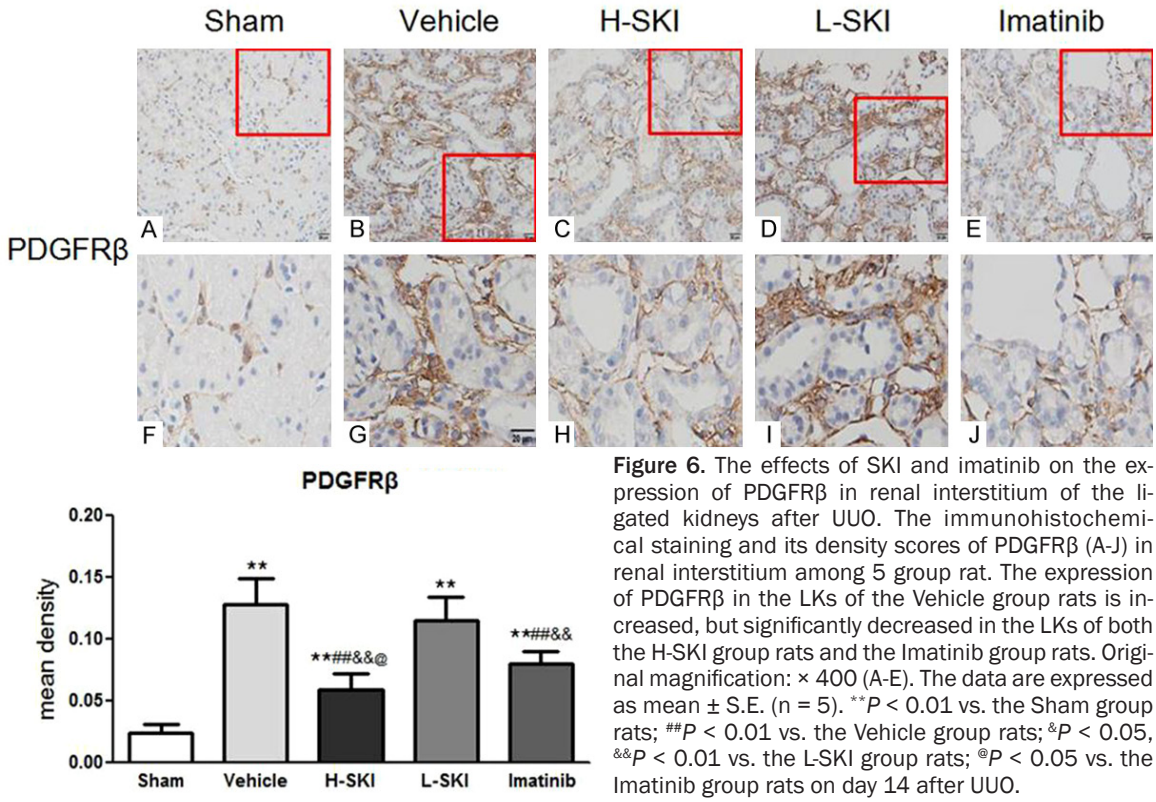

Figure 6. The effects of SKI and imatinib on the expression of PDGFRβ in renal interstitium of the ligated kidneys after UUO. The immunohistochemical staining and its density scores of PDGFRβ (A-J) in renal interstitium among 5 group rat. The expression of PDGFRβ in the LKs of the Vehicle group rats is increased, but significantly decreased in the LKs of both the H-SKI group rats and the Imatinib group rats. Original magnification: × 400 (A-E). The data are expressed as mean ± S.E. (n = 5). $^{**}P < 0.01$ vs. the Sham group rats; $^{\#\#}P < 0.01$ vs. the Vehicle group rats; $^{\&}P < 0.05$, $^{\&\&}P < 0.01$ vs. the L-SKI group rats; $^{@}P < 0.05$ vs. the Imatinib group rats on day 14 after UUO.

(**Figure 5U**, **5V**) were detected, respectively ($P < 0.05$), suggesting that the effects of H-SKI on attenuating TIF *in vivo* were superior to those of imatinib, which is an anti-fibrotic drug in the patients with nephrogenic systemic fibrosis in clinics.

Likewise, as shown in **Figures 6-8**, we also found that, compared with the NKs of the Sham group rats, the expressions of PDGFRβ (**Figure 6B**, **6G**), αSMA (**Figure 7B**, **7G**) and vimentin (**Figure 8B**, **8G**) were increased in peritubular pericytes, accompanied by the exasperation of TIF on day 14 after UUO, but significantly decreased in the LKs of both the H-SKI group rats (**Figures 6-8C** and **Figures 6-8H**) and the Imatinib group rats (**Figures 6-8E** and **Figures 6-8J**). And that, the statistical significant differences of these changes between the H-SKI group rats and the Imatinib group rats (**Figures 6-8**) were detected, respectively ($P < 0.05$), suggesting that the actions of H-SKI on inhibiting PMT *in vivo* were also superior to those of imatinib.

Here, noteworthily, consistent with the above-mentioned results, the expression of PDGFRβ as a key marker of PMT trigger [3] in the obstructed kidneys of the Vehicle group rats was increased (**Figure 6B**, **6G**), and markedly decreased in the H-SKI group rats (**Figure 6C**, **6H**). Despite these, we found in this study regrettably, after the short-term (28 days) drugs intervention, compared with the Vehicle group rats, except UNAG, the data of body weight (BW), ligated kidney weight (LKW), Scr, BUN, Alb and Upro in the UUO model rats on day 14 were not greatly altered in both the SKI-treated group rats and the imatinib-treated group rats (**Table 1**).

In brief, these results indicated that TIF was aggravated by PMT in the obstructed kidneys of the UUO model rats, and could be significantly improved by the high dose of SKI and imatinib *in vivo*, which were concretely reflected by inhibiting PDGFRβ, αSMA and vimentin expressions in peritubular pericytes and attenuating ECM accumulation and collagen deposition in renal interstitium.

PMT is blocked by SKI and imatinib through inhibiting the activation of PDGFR and VEGFR signaling after UUO

To demonstrate whether SKI could block PMT in the obstructed kidneys of the UUO model rats by likely inhibiting the activation of PDGFR

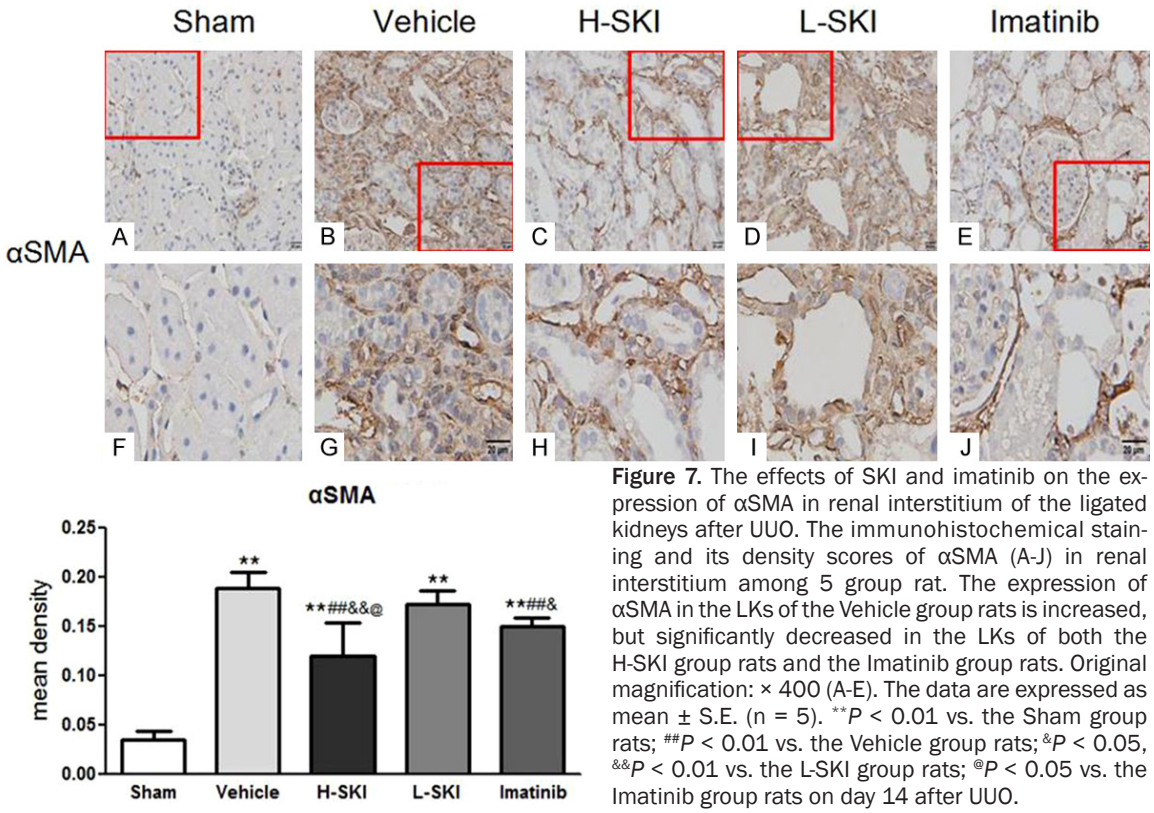

Figure 7. The effects of SKI and imatinib on the expression of αSMA in renal interstitium of the ligated kidneys after UUO. The immunohistochemical staining and its density scores of αSMA (A-J) in renal interstitium among 5 group rat. The expression of αSMA in the LKs of the Vehicle group rats is increased, but significantly decreased in the LKs of both the H-SKI group rats and the Imatinib group rats. Original magnification: × 400 (A-E). The data are expressed as mean ± S.E. (n = 5). $^{**}P < 0.01$ vs. the Sham group rats; $^{\#\#}P < 0.01$ vs. the Vehicle group rats; $^{\&}P < 0.05$, $^{\&\&}P < 0.01$ vs. the L-SKI group rats; $^{@}P < 0.05$ vs. the Imatinib group rats on day 14 after UUO.

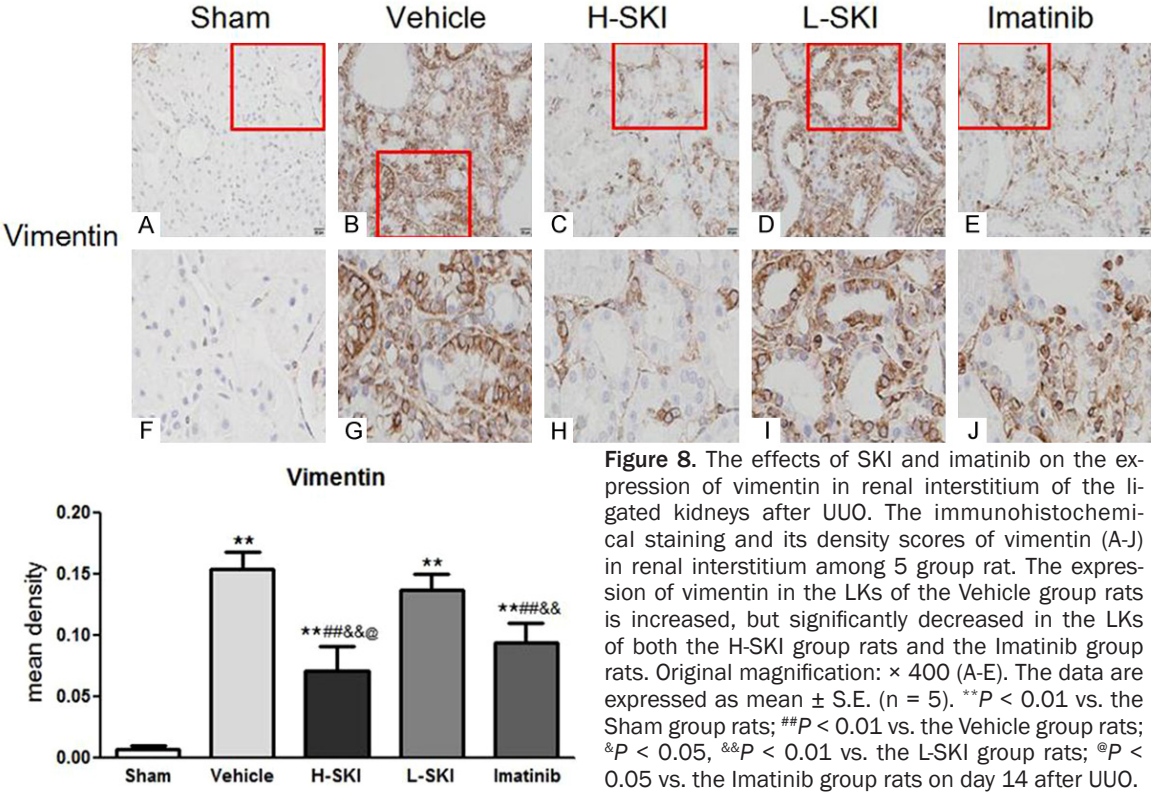

Figure 8. The effects of SKI and imatinib on the expression of vimentin in renal interstitium of the ligated kidneys after UUO. The immunohistochemical staining and its density scores of vimentin (A-J) in renal interstitium among 5 group rat. The expression of vimentin in the LKs of the Vehicle group rats is increased, but significantly decreased in the LKs of both the H-SKI group rats and the Imatinib group rats. Original magnification: × 400 (A-E). The data are expressed as mean ± S.E. (n = 5). $^{**}P < 0.01$ vs. the Sham group rats; $^{\#\#}P < 0.01$ vs. the Vehicle group rats; $^{\&}P < 0.05$, $^{\&\&}P < 0.01$ vs. the L-SKI group rats; $^{@}P < 0.05$ vs. the Imatinib group rats on day 14 after UUO.

signaling *in vivo*, we checked the regulative effects of the different doses of SKI, compared to a PDGFR tyrosine kinase inhibitor imatinib, on the protein expression levels of the pivotal

Table 1. BW, LKW and biochemical parameters in 5 group rats on day 14 after UUO (n = 5)

Group	Sham	Vehicle	H-SKI	L-SKI	Imatinib
BW (g)	360.6 ± 12.01	346.8 ± 14.20	347.6 ± 15.82	344.2 ± 11.08	350.4 ± 14.26
LKW (g)	1.53 ± 0.10	1.95 ± 0.238**	1.78 ± 0.22*	1.88 ± 0.18**	1.81 ± 0.16*
Scr (μmol/L)	22.4 ± 3.05	42.2 ± 4.21**	37.6 ± 3.85**	40.0 ± 4.06**	38.4 ± 4.28**
BUN (mmol/L)	5.70 ± 0.47	9.04 ± 0.70**	8.04 ± 0.92**	8.86 ± 0.86**	8.18 ± 0.89**
Alb (g/L)	33.26 ± 1.06	25.66 ± 1.45**	27.22 ± 0.96**	26.72 ± 1.19**	26.76 ± 1.28**
Upro (mg/d)	3.18 ± 0.50	22.88 ± 4.19**	20.56 ± 2.79**	22.82 ± 3.87**	20.72 ± 2.99**
UNAG (U/L)	5.92 ± 0.90	19.14 ± 1.41**	15.36 ± 1.27**,##,&&,@	18.00 ± 1.41**	17.16 ± 1.54**,#

Note: BW, body weight; LKW, ligated kidney weight; Scr, serum creatinine; BUN, serum blood urea nitrogen; Alb, albumin; Upro, 24 h urinary protein; UNAG, urinary *N*-acetyl-beta-*D*-glucosaminidase. *$P < 0.05$, **$P < 0.01$ vs. the Sham group rats. #$P < 0.05$, ##$P < 0.01$ vs. the Vehicle group rats. &&$P < 0.01$ vs. the L-SKI group rats. @$P < 0.05$ vs. the Imatinib group rats.

signaling molecules in PDGFR pathway in the LKs of the UUO model rats, such as PDGFRα, PDGFRβ, p-PDGFRα and p-PDGFRβ. Our data showed that the increased protein expression levels of PDGFRβ, PDGFRα, p-PDGFRβ and p-PDGFRα in the LKs of the UUO model rats were substantially down-regulated after the treatment with the high dose of SKI and imatinib. And that the statistical significant differences of these protein expression levels between the H-SKI group rats and the Imatinib group rats were detected, respectively ($P < 0.05$, $P < 0.01$) (**Figure 9A-D**), suggesting that the effect of H-SKI on inhibiting the activation of PDGFR signaling *in vivo* was superior to that of imatinib. In addition, noteworthily, by comparison with the Vehicle group rats, though the expression levels of the above-mentioned 4 proteins in the L-SKI group rats had a little change, the statistical significant differences between the L-SKI group rats and the Vehicle group rats were not found.

VEGFR signaling pathway has been also identified as the regulator of PMT [12]. Therefore, we next examined the protein expression levels of VEGFR2 and its ligand VEGFA in the obstructed kidneys of the UUO model rats, which are the key signaling molecules in VEGFR pathway. As also shown in **Figure 9**, the protein expression levels of VEGFR2 and VEGFA were strikingly up-regulated in the LKs of the Vehicle group rats, and alleviated significantly in the H-SKI group rats and the Imatinib group rats respectively. However, the statistical significant difference of VEGFR2 protein expression level between the H-SKI group rats and the Imatinib group rats was only detected ($P < 0.05$) (**Figure 9E**), suggesting that the effect of SKI at the high dose on suppressing the activation of VEGFR signaling *in vivo* was also superior to that of imatinib.

In sum, these results indicated that SKI and imatinib could specifically block PMT in the obstructed kidneys of the UUO model rats through inhibiting the activation of PDGFR and VEGFR signaling, which were concretely shown by down-regulating the protein expression levels of PDGFRβ, PDGFRα, p-PDGFRβ, p-PDGFRα, VEGFR2 and VEGFA in the kidney. Furthermore, the effects of SKI at the high dose were partially superior to those of imatinib.

Discussion

In the present study, using the UUO model rats, we demonstrated that PMT trigger was persistently accompanied with TIF exasperation in the obstructed kidneys after UUO, and that SKI, a modern intravenous preparation of Chinese patent medicine, could definitely target PMT and significantly diminish TIF *in vivo*. In addition, the high dose of SKI, superior to imatinib as an anti-fibrotic drug in clinics, could specifically block PMT through inhibiting the activation of PDGFR and VEGFR signaling in the kidneys. These results suggested that the intervention of PMT and its signaling activation by the continuous administration of SKI leads to the impressive renoprotection after the obstructed renal injury. To the best of our knowledge, it is the first study to report that targeting PMT is capable of improving the artificial TIF in the field of TCM therapeutics.

In this study, we were firstly interested in the pathomorphological characteristics related to renal interstitial damage induced by UUO and whether could be ameliorated by the drugs *in vivo* within a short time (28 days). Ai *et al*. [23] reported that the obstructed kidneys at day 7 after UUO revealed the typical features of ON, such as tubular degeneration and atrophy,

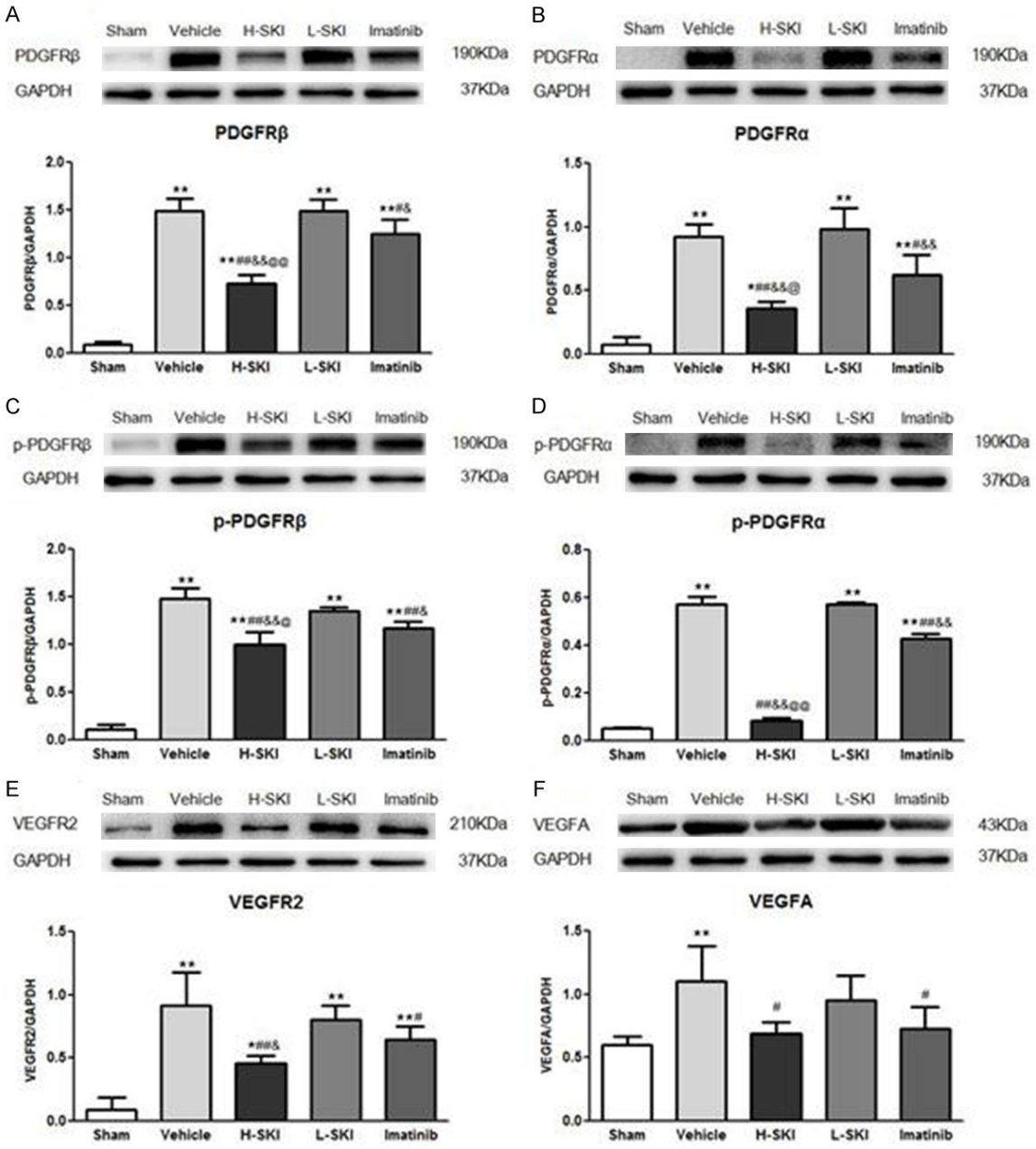

Figure 9. The effects of SKI and imatinib on the protein expression levels of PDGFRβ, PDGFRα, p-PDGFRβ, p-PDGFRα, VEGFR2 and VEGFA in the ligated kidneys after UUO. The protein expression levels of PDGFRβ (A), PDGFRα (B), p-PDGFRβ (C), p-PDGFRα (D), VEGFR2 (E) and VEGFA (F) among 5 group rats. The increased protein expression levels of PDGFRβ, PDGFRα, p-PDGFRβ, p-PDGFRα, VEGFR2 and VEGFA in the LKs of the UUO model rats are substantially down-regulated after the treatment with the high dose of SKI and imatinib. The data are expressed as mean ± S.E. (n = 5). $^{*}P < 0.05$, $^{**}P < 0.01$ vs. the Sham group rats; $^{\#}P < 0.05$, $^{\#\#}P < 0.01$ vs. the Vehicle group rats; $^{\&}P < 0.05$, $^{\&\&}P < 0.01$ vs. the L-SKI group rats; $^{@}P < 0.05$, $^{@@}P < 0.01$ vs. the Imatinib group rats on day 14 after UUO.

interstitial fibrosis and inflammatory cell infiltration in renal interstitium. In agreement with this investigation, we also found the analogous alterations and related abnormal biochemical parameters including Scr, BUN, Upro and UNAG, which were detected and peaked at day 7 after obstruction (data not shown). On day 14 after UUO, the persistent TIF was induced in the LKs of the UUO model rats, concretely characterized by tubular atrophy, ECM accumulation and collagen deposition in renal interstitium. Meanwhile, fibrotic markers FN and CIV exhibited the

intense expressions in renal interstitial area. Fortunately, besides interstitial inflammatory cell infiltration, the above-mentioned major interstitial pathomorphological changes and the increased UNAG (renal tubular injurious marker) were significantly ameliorated after the continuous treatment (28 days) with the high dose of SKI or imatinib, respectively. Consequently, we considered that this ON rat model should be useful in unraveling the pathogenesis of TIF. More importantly, based on this established rat model, it is possible to prove the anti-fibrotic effects of the drugs *in vivo* within the limited time.

The previous studies reported that SKI at a low dose could suppress renal fibrosis and oxidative stress in 5/6 nephrectomized rats [18]. By comparison, in this study, using a classical ON model induced by UUO, we further investigated the dose effects of SKI on TIF *in vivo*, compared with imatinib as an anti-fibrotic drug in clinics [22]. Our data definitely indicated that SKI at the high dose of 5 g/kg daily slightly improved ECM accumulation, collagen deposition and FN and CIV expressions in renal interstitium of the LKs in the UUO model rats. Furthermore, the beneficial effects of SKI at the high dose on the obstructed renal injuries were better than those of the low dose of SKI and imatinib. We thus confirmed that SKI could dose-dependently ameliorate TIF *in vivo*. Nonetheless, our results showed that the abnormal data of BW, LKW, Scr, BUN, Alb, Upro and interstitial inflammatory cell infiltration in the LKs of the UUO model rats on day 14 were not obviously changed after the treatment with SKI or imatinib within the short-term (28 days) drugs intervention. For these reasons, a long time of SKI treatment should be necessary in future studies to testify the comprehensive actions of SKI *in vivo*.

For all we know, in rodent ON models, the overexpressions of TGF-β1 and Smad proteins in the resident fibroblasts are closely related with fibrosis [8]. Hence, it seems reasonable to hypothesize that aiming at TGF-β1/Smad signaling pathway, SKI at the high dose may provide a quick and effective treatment for TIF *in vivo*. However, what is intriguing that, in this study, we could not find the significant alteration of signaling molecules including TGF-β1, Smad2/3, Smad4 and Smad7 (data not shown) after drugs administration, suggesting that other molecular mechanism might be involved in the treatment of SKI for TIF in this UUO model.

Recently, the growing evidences have manifested that renal pericytes as another major source of myofibroblasts are activated to lead to microvascular rarefaction and TIF [1, 3-8]. During the process of transition from pericytes to myofibroblasts in the kidney, some of the best-described markers used to identify pericytes include PDGFRβ and αSMA. In which, PDGFRβ as one of the most widely used pericyte markers plays a key role in pericyte recruitment, investment and maturation of the microvasculature [4]; αSMA as an intracellular marker is restricted to be expressed by the activated pericytes at sites of vascular remodeling, also by myofibroblasts and smooth muscle cells [29]. In addition, vimentin as a marker of myofibroblasts has been widely recognized [30]. Therefore, the trigger of PMT can be marked by the over-expressions of PDGFRβ, αSMA and vimentin at peritubular pericytes. Our results distinctly showed that the expression levels of PDGFRβ, αSMA and vimentin were up-regulated at peritubular pericytes, accompanied by the exasperation of TIF in the UUO model rats, and significantly down-regulated after the treatment with the high dose of SKI or imatinib, suggesting that the triggered PMT in the obstructed kidneys of the UUO model rats could be obviously inhibited by the high dose of SKI and imatinib *in vivo*.

A series of studies conducted by Lin *et al*. have identified that PDGFR signaling pathway plays a key role in PMT trigger and will be the therapeutic molecular target to prevent microvascular rarefaction and TIF *in vivo* [3, 12]. Chen *et al*. [3] reported that PDGFRα and PDGFRβ are expressed exclusively at interstitial pericytes and myofibroblasts. PDGFR expression is increased markedly at the injurious tubules after UUO. When the activation of PDGFRα or PDGFRβ is inhibited by the receptor-specific antibody in mice following the obstructed renal damage, PMT is decreased and the related signaling molecules including p-PDGFRα and p-PDGFRβ are suppressed. Hence, it is considered that PDGFR signaling is the upstream regulative pathway of PMT trigger. Corresponding to this, we also found in this study that the increased protein expression levels of PDGFRβ, PDGFRα, p-PDGFRβ and p-PDGFRα in the kidneys of the UUO model rats were substantially

down-regulated after the treatment with the high dose of SKI and imatinib. Here, interestingly, the suppressive effect of SKI at the high dose on the activation of PDGFR signaling was significantly superior to PDGFR tyrosine kinase inhibitor imatinib, which could specifically inhibit pericytes proliferation and TIF in fibrogenic model of UUO [31].

It has been reported that the activation of VEGFR is a critical signaling pathway that links endothelial cells with pericytes. Blocking VEGFR signaling leads to the attenuation of TIF and the down-regulation of profibrotic cytokines including PDGF and TGF-β1 [12]. Thus, the activation of VEGFR at endothelial cells drives PMT and aggravates TIF [10]. Our results clearly displayed that the protein expression levels of VEGFR2 and VEGFA (the ligand for VEGFR2) were strikingly up-regulated in the LKs of the UUO model rats, and alleviated significantly after the treatment with the high dose of SKI and imatinib. However, notice that the effects of SKI at the high dose on suppressing the activation of VEGFR signaling were superior to imatinib.

In summary, we clarified in this report that the high dose of SKI, superior to imatinibas as an anti-fibrotic drug in clinics, could attenuate TIF *in vivo* through blocking PMT and inhibiting the activation of PDGFR and VEGFR signaling in the kidneys of the UUO model rats. These findings may partly explain the therapeutic mechanisms of SKI in treating TIF of ON patients in clinic, and further suggest that targeting PMT can provide new strategies for ON treatment.

Acknowledgements

This work was supported by 2 grants from the National Natural Science Foundation of China (81573903 and 81603675), a grant from Nanjing Medical Science and Technique Development Foundation (QRX17042) and 2 grants from the Key Science and Technology Development Program of Nanjing City of the People's Republic of China (YKK15057 and YKK16097). The authors thank Dr. Xunyang Luo and Dr. Le Zhang (Department of Laboratory Medicine, Nanjing Drum Tower Hospital, The Affiliated Hospital of Nanjing University Medicine School, Nanjing, China) for their technical assistance and instructions. The authors also thank Prof. Jian Yao (Division of Molecular Signaling, Department of Advanced Biomedical Research, Interdisciplinary Graduate School of Medicine and Engineering, University of Yamanashi, Yamanashi, Japan) for his helpful discussions.

Disclosure of conflict of interest

None.

Abbreviations

Alb, albumin; αSMA, α-smooth muscle actin; BUN, blood urea nitrogen; BW, body weight; CIV, collagen type IV; CKD, chronic kidney disease; CRF, chronic renal failure; FN, fibronectin; LKs, ligated kidneys; LKW, ligated kidney weight; NKs, normal kidneys; NLKs, non-ligated kidneys; PDGF, platelet-derived growth factor; PDGFR, PDGF receptor; p-PDGFRα, phosphorylated PDGFRα; p-PDGFRβ, phosphorylated PDGFRβ; Scr, serum creatinine; SKI, Shenkang injection; TCM, traditional Chinese medicine; TGF-β, transforming growth factor-β; TIF, tubulointerstitial fibrosis; UNAG, urinary *N*-acetyl-beta-*D*-glucosaminidase; Upro, 24 h urinary protein; UUO, unilateral ureteral obstruction; VEGF, vascular endothelial growth factor; VEGFR, VEGF receptor; WB, Western blot.

Address correspondence to: Dr. Yigang Wan, Department of Traditional Chinese Medicine (TCM), Nanjing Drum Tower Hospital, The Affiliated Hospital of Nanjing University Medical School, 321 Zhongshan Road, Nanjing 210008, China. E-mail: wyg68918@hotmail.com; Dr. Dongwei Cao, Department of Nephrology, Nanjing Drum Tower Hospital, The Affiliated Hospital of Nanjing University Medical School, 321 Zhongshan Road, Nanjing 210008, China. E-mail: cdwlqq@hotmail.com

References

[1] Liu Y. Cellular and molecular mechanisms of renal fibrosis. Nat Rev Nephrol 2011; 7: 684-696.

[2] Tan RJ, Zhou D and Liu Y. Signaling crosstalk between tubular epithelial cells and interstitial fibroblasts after kidney injury. Kidney Dis (Basel) 2016; 2: 136-144.

[3] Chen YT, Chang FC, Wu CF, Chou YH, Hsu HL, Chiang WC, Shen J, Chen YM, Wu KD, Tsai TJ, Duffield JS and Lin SL. Platelet-derived growth factor receptor signaling activates pericyte-myofibroblast transition in obstructive and post-ischemic kidney fibrosis. Kidney Int 2011; 80: 1170-1181.

[4] Lin SL, Kisseleva T, Brenner DA and Duffield JS. Pericytes and perivascular fibroblasts are the primary source of collagen-producing cells in obstructive fibrosis of the kidney. Am J Pathol 2008; 173: 1617-1627.
[5] Shaw I, Rider S, Mullins J, Hughes J and Péault B. Pericytes in the renal vasculature: roles in health and disease. Nat Rev Nephrol 2018; 14: 521-534.
[6] Smith SW, Chand S and Savage CO. Biology of the renal pericyte. Nephrol Dial Transplant 2012; 27: 2149-2155.
[7] Sun YB, Qu X, Caruana G and Li J. The origin of renal fibroblasts/myofibroblasts and the signals that trigger fibrosis. Differentiation 2016; 92: 102-107.
[8] Wu CF, Chiang WC, Lai CF, Chang FC, Chen YT, Chou YH, Wu TH, Linn GR, Ling H, Wu KD, Tsai TJ, Chen YM, Duffield JS and Lin SL. Transforming growth factor β-1 stimulates profibrotic epithelial signaling to activate pericyte-myofibroblast transition in obstructive kidney fibrosis. Am J Pathol 2013; 182: 118-131.
[9] Schrimpf C, Xin C, Campanholle G, Gill SE, Stallcup W, Lin SL, Davis GE, Gharib SA, Humphreys BD and Duffield JS. Pericyte TIMP3 and ADAMTS1 modulate vascular stability after kidney injury. J Am Soc Nephrol 2012; 23: 868-883.
[10] Chang FC, Chou YH, Chen YT and Lin SL. Novel insights into pericyte-myofibroblast transition and therapeutic targets in renal fibrosis. J Formos Med Assoc 2012; 111: 589-598.
[11] Floege J, Eitner F and Alpers CE. A new look at platelet-derived growth factor in renal disease. J Am Soc Nephrol 2008; 19: 12-23.
[12] Lin SL, Chang FC, Schrimpf C, Chen YT, Wu CF, Wu VC, Chiang WC, Kuhnert F, Kuo CJ, Chen YM, Wu KD, Tsai TJ and Duffield JS. Targeting endothelium-pericyte cross talk by inhibiting VEGF receptor signaling attenuates kidney microvascular rarefaction and fibrosis. Am J Pathol 2011; 178: 911-923.
[13] Du J, Cheng BC, Fu XQ, Su T, Li T, Guo H, Li SM, Wu JF, Yu H, Huang WH, Cao H and Yu ZL. In vitro assays suggest Shenqi Fuzheng Injection has the potential to alter melanoma immune microenvironment. J Ethnopharmacol 2016; 194: 15-19.
[14] Pang LZ, Ju AC, Zheng XJ, Li F, Song YF, Zhao Y, Gu YF, Chen FL, Liu CH, Qi J, Gao Z, Kou JP and Yu BY. YiQiFuMai powder injection attenuates coronary artery ligation-induced myocardial remodeling and heart failure through modulating MAPKs signaling pathway. J Ethnopharmacol 2017; 202: 67-77.
[15] Lian JP, Shan H, Fang ZY, Li XC and Zuo Y. Effects of Shenkang injection on chronic renal failure: a meta-analysis. Chin Tradit Pat Med (in Chinese) 2015; 37: 1677-1682.
[16] Xu T, Zuo L, Sun Z, Wang P, Zhou L, Lv X, Jia Q, Liu X, Jiang X, Zhu Z, Kang J and Zhang X. Chemical profiling and quantification of ShenKang injection, a systematic quality control strategy using ultra high performance liquid chromatography with Q Exactive hybrid quadrupole orbitrap high-resolution accurate mass spectrometry. J Sep Sci 2017; 40: 4872-4879.
[17] Yao S, Zhang J, Wang D, Hou J, Yang W, Da J, Cai L, Yang M, Jiang B, Liu X, Guo DA and Wu W. Discriminatory components retracing strategy for monitoring the preparation procedure of Chinese patent medicines by fingerprint and chemometric analysis. PLoS One 2015; 10: e0121366.
[18] Liu M, Park J, Wu X, Li Y, Tran Q, Mun K, Lee Y, Hur GM, Wen A and Park J. Shen-Kang protects 5/6 nephrectomized rats against renal injury by reducing oxidative stress through the MAPK signaling pathways. Int J Mol Med 2015; 36: 975-984.
[19] Wu X, Guan Y, Yan J, Liu M, Yin Y, Duan J, Wei G, Hu T, Weng Y, Xi M and Wen A. ShenKang injection suppresses kidney fibrosis and oxidative stress via transforming growth factor-β/Smad3 signalling pathway in vivo and in vitro. J Pharm Pharmacol 2015; 67: 1054-1065.
[20] Zhang YU, Zhou N, Wang H, Wang S and He J. Effect of Shenkang granules on the progression of chronic renal failure in 5/6 nephrectomized rats. Exp Ther Med 2015; 9: 2034-2042.
[21] Xu S, Lv Y, Zhao J, Wang J, Zhao X and Wang S. Inhibitory effects of Shenkang injection and its main component emodin on the proliferation of high glucose-induced renal mesangial cells through cell cycle regulation and induction of apoptosis. Mol Med Rep 2016; 14: 3381-3388.
[22] Elmholdt TR, Buus NH, Ramsing M and Olesen AB. Antifibrotic effect after low-dose imatinib mesylate treatment in patients with nephrogenic systemic fibrosis: an open-label non-randomized, uncontrolled clinical trial. J Eur Acad Dermatol Venereol 2013; 27: 779-784.
[23] Ai J, Nie J, He J, Guo Q, Li M, Lei Y, Liu Y, Zhou Z, Zhu F, Liang M, Cheng Y and Hou FF. GQ5 hinders renal fibrosis in obstructive nephropathy by selectively inhibiting TGF-β-induced Smad3 phosphorylation. J Am Soc Nephrol 2015; 26: 1827-1838.
[24] Huang YR, Wei QX, Wan YG, Sun W, Mao ZM, Chen HL, Meng XJ, Shi XM, Tu Y and Zhu Q. Ureic clearance granule, alleviates renal dysfunction and tubulointerstitial fibrosis by promoting extracellular matrix degradation in renal failure rats, compared with enalapril. J Ethnopharmacol 2014; 155: 1541-1552.

[25] Tu Y, Sun W, Wan YG, Gao K, Liu H, Yu BY, Hu H and Huang YR. Dahuang fuzi decoction ameliorates tubular epithelial apoptosis and renal damage via inhibiting TGF-β1-JNK signaling pathway activation in vivo. J Ethnopharmacol 2014; 156: 115-124.

[26] Wan YG, Che XY, Sun W, Huang YR, Meng XJ, Chen HL, Shi XM, Tu Y, Wu W and Liu YL. Low-dose of multi-glycoside of *Tripterygium wilfordii* Hook. f., a natural regulator of TGF-β1/Smad signaling activity improves adriamycin-induced glomerulosclerosis in vivo. J Ethnopharmacol 2014; 151: 1079-1089.

[27] Tu Y, Gu L, Chen D, Wu W, Liu H, Hu H, Wan Y and Sun W. Rhein inhibits autophagy in rat renal tubular cells by regulation of AMPK/mTOR signaling. Sci Rep 2017; 7: 43790.

[28] Wan YG, Zhao Q, Sun W, Zhang HL, Li M, Wei QX, Wu W, Yue LJ and Wang Q. Contrasting dose-effects of multi-glycoside of *Tripterygium wilfordii* HOOK. f. on glomerular inflammation and hepatic damage in two types of anti-Thy1.1 glomerulonephritis. J Pharmacol Sci 2012; 118: 433-446.

[29] Hellberg C, Ostman A and Heldin CH. PDGF and vessel maturation. Recent Results Cancer Res 2010; 180: 103-114.

[30] Rodríguez-Peña AB, Grande MT, Eleno N, Arévalo M, Guerrero C, Santos E and López-Novoa JM. Activation of Erk1/2 and Akt following unilateral ureteral obstruction. Kidney Int 2008; 74: 196-209.

[31] Kumar V, Kamal R and Sharma V. Heterocyclic analogues as kinase inhibitors: a focus review. Curr Top Med Chem 2017; 17: 2482-2494.

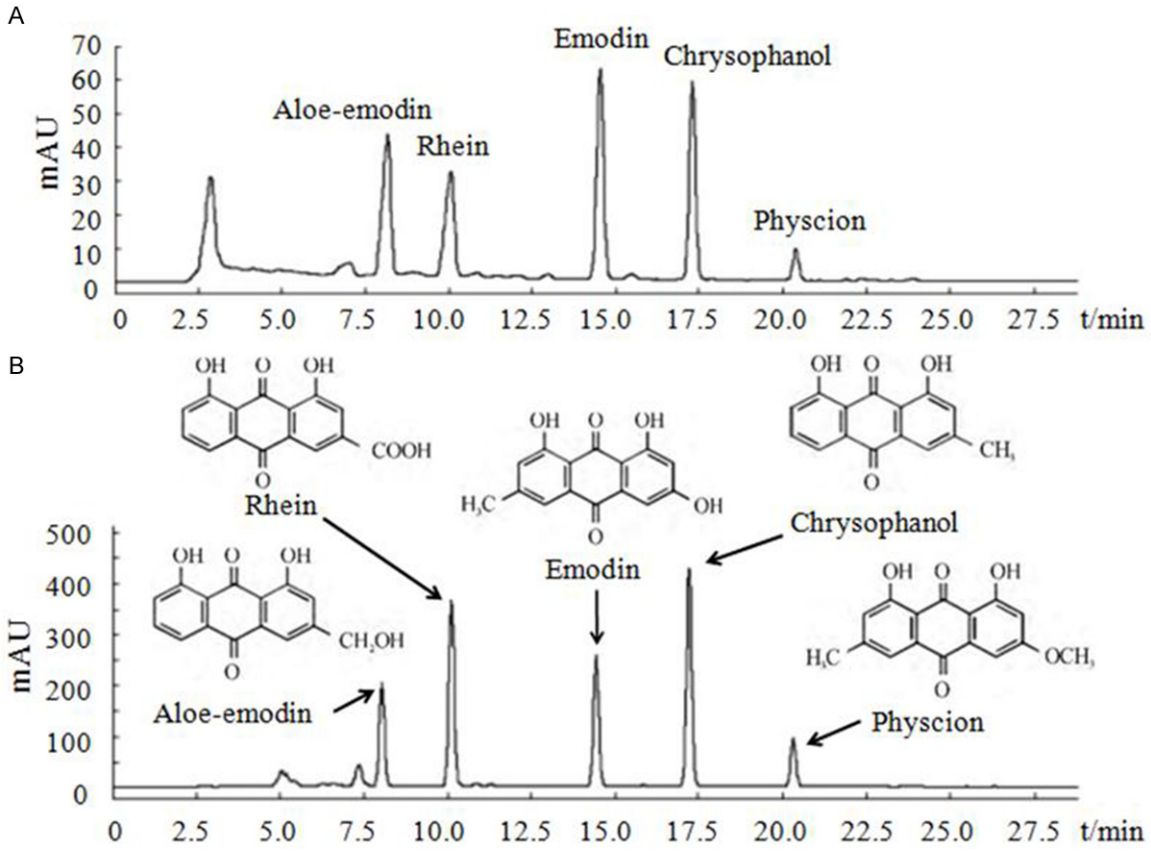

Figure S1. Fingerprint analysis of SKI by HPLC. A. The chromatograms of mixed standards. B. The samples of SKI.

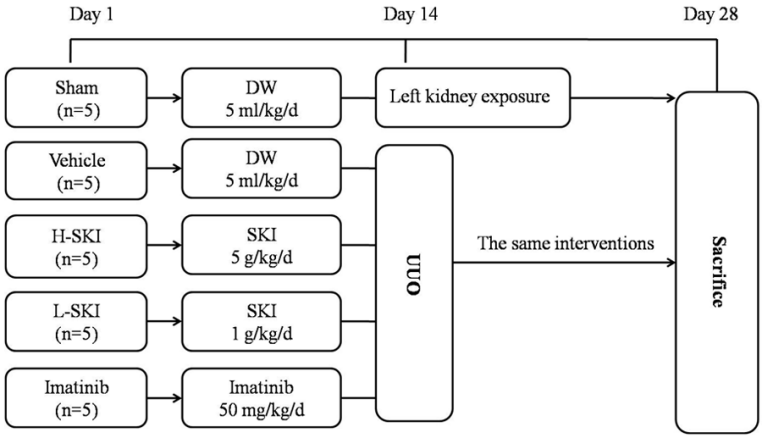

Figure S2. Experimental procedure.